Published by :
http://www.ijert.org

International Journal of Engineering Research & Technology (IJERT)
ISSN: 2278-0181
Vol. 11 Issue 07, July-2022

Design and Development of a Cooling System for A Vaccine Container by using Vortex Tube Refrigeration

Sagar Manmath Swami[1]
M. Tech. Student
Mechanical Engineering Department
Sardar Patel College of Engineering, Andheri (West)
Mumbai, Maharashtra, India

Prof. Kunal Y. Bhavsar[2]
Mechanical Engineering Department,
Sardar Patel College of Engineering, Andheri (West)
Mumbai, Maharashtra, India

***Abstract*—While dealing with the daily challenges of the COVID-19 pandemic, everyone is looking to science for a solution in the form of effective vaccine preservation in transportation. According to studies, temperature changes in vaccine storage cause up to 10% of vaccinations to be lost during transport. Especially in rural areas where electricity is relatively limited, making it difficult to maintain the ideal temperature range of 2°C to 8°C for vaccine preservation. This vortex tube refrigeration system includes a vortex tube, a cold box, a compressed air storage tank, compressed air hoses and a cooling coil. In this paper, the parametric analysis of a vortex tube is performed in ANSYS Fluent based on the cooling load calculations. Operating conditions of a vortex tube are optimized, for energy saving, where minimum inlet air pressure of 4 bar, and a cold flow rate is adjusted by a conical control valve near the hot exit of a vortex tube for the required temperature of 276K, which is the input for the cold box. Following that, the length of the cooling coil is estimated and based on the ANSYS Fluent flow analysis of the coil, the most optimum spiral design for the lowest possible temperature and pressure loss for the cooling coil is proposed.**

Keywords*—Vaccine Container; Vortex Tube; Refrigeration; Computational-Fluid Dynamics

I. INTRODUCTION

Up to 10% of vaccines can be lost in transit due to temperature changes required for preservation. Vaccines include sensitive biological molecules that can be irreversibly destroyed by extremes of heat and cold. As a result, it's critical to keep a close eye on vaccination temperature throughout its life cycle. Organs and vaccines are frequently stored and transported in thermal containers. In distant areas, where electricity is unavailable, these areas require consistent long-term refrigeration to maintain the ideal temperature range of 2 to 8°C for vaccines in India. The requisite temperature conditions are normally maintained for 6 (at best, 12) hours in light, compact containers [1].

Using vortex tube refrigeration, several researchers have offered a number of ideas.

Authors S. G. Voronchikhin1 and M. A. Tuev [1], proposed the prospect of using the vortex effect in a transportable thermostatic unit. The temperature of the effective volume and its contents is determined by the airflow pressure in the pipe. As a biological item, test tubes with 200 mL of blood at 23°C were used to prove this. T. Karthikeya Sharma, G. Amba Prasad Rao, and K. Madhu Murthy [2], evaluated the energy separation in a vortex tube. Additionally, they applied and evaluated turbulence models such as LES and k–ε, k–ω and used CFD confidently throughout a wide range of operating conditions and geometries. G. F. Nellis, and S. A. Klein [3], have studied the potential performance benefit of replacing a refrigeration system's throttling valve with a properly adjusted vortex tube. Xiaojie Zhai [4] discusses the vortex tube refrigeration theory which is used to study mine cooling jacket. It utilized compressed exhaust gas as a gas source, which solves the problem of large-scale cooling equipment that relies on energy while also avoiding the emission of harmful gases. This demonstrates that the vortex tubes kind of mine cooling jacket can retain the work's fundamental stability. According to Akash S. Bidwaik and Sumit Mukund Dhavale's [5] experimental findings, the temperature drop is inversely proportional to input pressure intensity; the higher the inlet pressure, the greater the temperature drop at the cold exit. Also B. Sreenivasa Kumar Reddy and Prof. K. Govindarajulu [9], developed a vortex tube refrigeration-based vehicle air conditioning system that is more affordable and energy-efficient than a traditional air conditioning system. The aforementioned literature study presents a cooling system that uses vortex tube refrigeration for numerous purposes. They were able to develop self-sustaining units by utilizing vortex tube refrigeration.

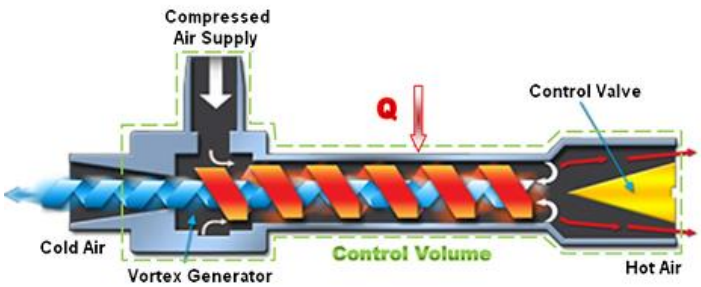

Fig. 1 Schematic diagram of Counterflow vortex tube [2]

This review of the literature reveals tremendous progress in our understanding of the vortex tube, which was mainly driven by experimental research and some numerical analysis work. These literature reviews served as the motivation for the present work, which sought to develop a vortex tube-based cooling system for vaccination containers.

International Journal of Engineering Research & Technology (IJERT)
ISSN: 2278-0181
Vol. 11 Issue 07, July-2022

II. METHODOLOGY

A. *Selection of Vaccine Container as per the requirement.*

The size (volume) and other specifications of modern thermal containers vary as per the applications and requirements. For this study, a lightweight, small-volume container from Nilkamal model RCB 503L with a gross volume of 23.3 L is selected. This sort of thermal container is passive, meaning that its main purpose is to keep the stored biological material cool. The cold box's external surface is made of LLDPE (Linear low-density polyethylene) thickness (Xi) varies as per the side of the cold box ranging from 6mm to 13mm and the inside insulation is CFC-free polyurethane with a thickness of 111mm and thermal conductivity of (λi) 0.035(W/mK). With that this cold box can provide the required temperature conditions for up to 96 hours.

Fig. 2. Cold box RCB 503L [23].

B. *Calculation of Cooling Load for Cold Box RCB 503L.*

Calculating the cooling load of the cold box determines heat intake. As a result of that, the required refrigeration capacity is established to match the calculated cooling load, allowing for optimal vortex tube selection.

- External Dimensions of the cold box = 0.774(L) x 0.616 (W) x 0.530(H)m,
- Inner Dimensions of the cold box = 0.528(L) x 0.382 (W) x 0.282(H)m,
- The outside temperature (T_o) can be the ambient temperature where the box will be kept is 318k (taking maximum).
- The inside temperature (T_i) will be decided by the vaccine requirement of 276K (in between 2°C to 8°C) (taking the minimum).

1) Transmission heat load (H_1):

Calculations of Heat conducted through the walls of the cold box:

Where, Q_c is heat transmission at the flat surface (W), U is

$$Q_c = UA\,(T_o - T_i) \quad (1)$$

$$\frac{1}{U} = \frac{1}{\alpha i} + \sum_{i=1}^{n} \frac{Xi}{\lambda i} + \frac{1}{\alpha_o} \quad (2)$$

total heat transmission coefficient (W/m^{2}K), area (A) of heat transmission (m^2), coefficient of heat transmission of inside (αi), and outside (αo) surfaces are 6 W/m^{2}K and 45 W/m^{2}K respectively.

The overall transmission load of all six walls is calculated as 33.0444W, with a 10% allowance (for each side) taken into account as a precautionary measure in the form of heat infiltration from unidentified sources.

2) Infiltration heat (H_2):

The thermal infiltration load comes mainly from the entry of hot air into the cold box in the event of a door opening or structural deformation such as wall fractures in the cold box RCB 503L that contribute to small leakage.

$$H_2 = z \times V \times \frac{1}{v} \times \Delta h \quad (3)$$

Where, volume of the cold storage (V) is calculated using the internal dimensions of the cool box RCB 503L [25]. The reference value for the total number of air exchanges (z) in this scenario is taken as 5 [23]. And the specific volume of air at 45°C and 60% relative humidity is calculated as 0.9 m3/kg. In this case, h1 and h2 are 142 Kj/kg and 15 Kj/kg, respectively.

3) Total heat (H_3):

$$H_3 = H_1 + H_2 \quad (4)$$

The refrigeration system only after considering the safety factor of 15%, and the total refrigeration capacity is determined as 84.087W.

C. *Selection of Vortex Tube.*

Vortex Tubes from Exair Corporation are a low-cost, reliable and maintenance-free solution to industrial spot cooling problems. Based on the calculated cooling load of 84.087W, the overall refrigeration capacity is determined to be 286.9167 BTU/hr. Temperatures, and cooling power may very well be adjusted to produce temperatures ranging from -46°C to 127°C. for this study Vortex tube model 3208 with a cooling load capability of up to 550 Btu/hr is selected, for the cold box RCB 503L. In comparison to calculations, this vortex tube model 3208 have higher refrigeration capacity.

Fig. 3. EXAIR Vortex Tube model 3208 [20].

D. *Numerical methodology of vortex tube analysis.*

The essential requirement in this research work is to achieve 276K at the cold end while maintaining a low temperature and pressure loss. For that, the present study focuses on optimizing the design of a vortex tube model 3208 by utilizing design parameters (such as the number of nozzles, and control valve settings) as well as operational parameters (like varying input stagnation pressures, mass fractions and temperatures at the cold and hot end, etc.) based on the design criteria. This research work is carried out by using the ANSYS

International Journal of Engineering Research & Technology (IJERT)
ISSN: 2278-0181
Vol. 11 Issue 07, July-2022

Fluent 2021R2 finite volume-based solver to solve the governing equations and the boundary conditions.

1) Geometry Modeling

Fig. 4 shows the schematic diagram and the dimensions of the vortex tube under study. A geometric model of the vortex tube with 2, 4, and 6 number of inlet nozzles were considered, as shown in Fig. 5, and the following geometrical parameters are taken into account based on manufacturing data and research for optimal performance.

- D = 9.5 mm, L/D < 8.21 [26], where L is length and D is the diameter of the vortex tube;
- The total relative area of inlet tubular nozzles A_i/A is equal to 0.14;
- $A_c/A = 0.44$ is the cold air relative exit area [24];
- The ring-shaped relative hot air outflow area $A_{ho}/A = 0.052$, where A_{ho} is the area of the hot outlet and Ac is the area of the cool outlet [25];
- In addition, for Conical control valves with diameter $D_1/D = 0.667$ [25].

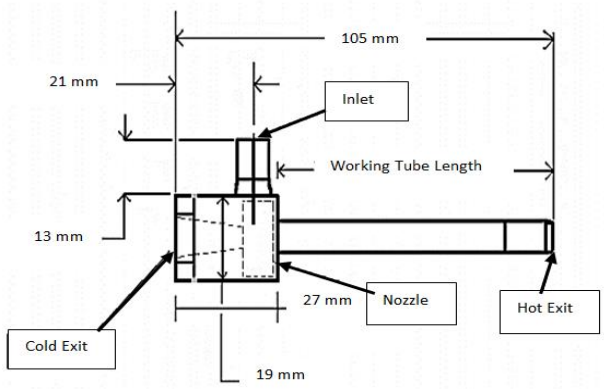

Fig. 4. Specifications of the Vortex Tube model 3208

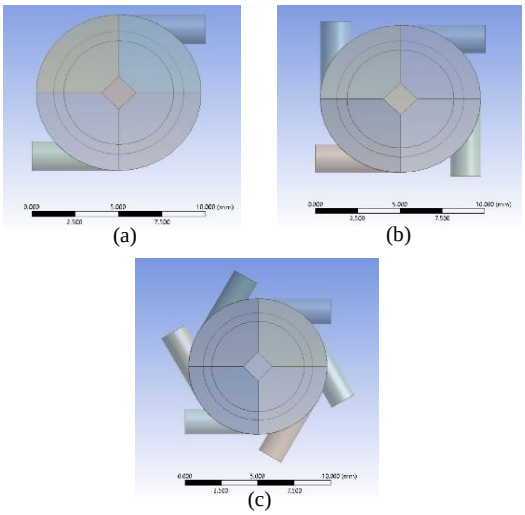

Fig. 5 Geometry of (a) Case1 (b) Case2 and (c) Case3.

As illustrated in Fig. 5, there are primarily three cases based on the number of nozzles (2, 4, and 6) that are taken into consideration for the flow and temperature analysis of the vortex tube. Each of these cases is further subdivided into several subcases depending on the air inlet pressure (3bar, 4bar, 5 bar, and 7bar).

2) Meshing model

The ANSYS mesh 2021R2 workbench has its own meshing tool. The mesh is created using hexahedral volumes and wedges. Along with face meshing and body sizing, inflation is applied to all boundaries, including nozzle inlets, hot and cold outlets, and so on. To increase the number of cells, the sizing option is also used with element sizes of 0.4 mm. As a result, the final mesh created is a structured mesh with boundary inflation.

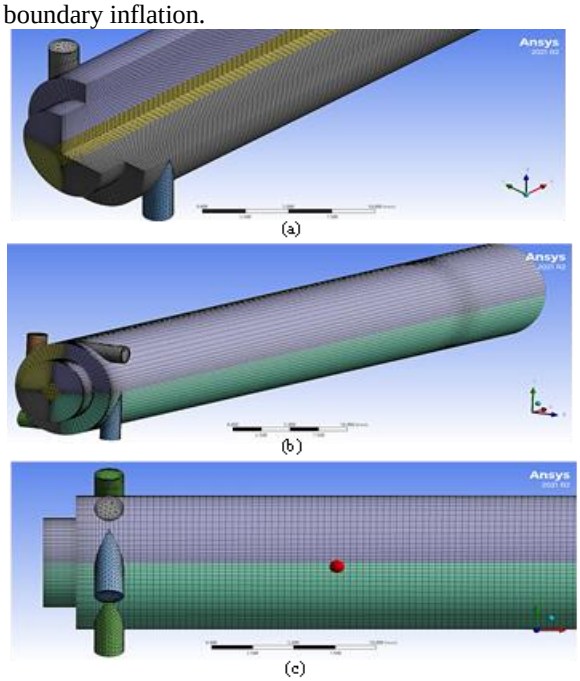

Fig. 6. Structured mesh on - (a) Case 1 with 2 nozzles, (b) Case 2 with 4 nozzles and (c) Case 3 with 6 nozzles.

3) Mathematical Modelling

The flow entering the vortex tube changes velocity from subsonic to sonic, resulting in a significant change in density. Therefore, a compressible flow model is used. The available pressure gradient causes the flow structure to form inside the vortex tube. It is clear that the phenomena of energy separation are not caused by any external energy interaction. Instead, it is merely a redistribution of energy associated only with entering compressed flow. The energy equation and the equation of an ideal gas are used to analyze variations in density in the flow field and temperature distribution. To develop a mathematical model for the current problem, the following assumptions are made.

- The working medium is an ideal gas,
- The vortex tube wall is considered adiabatic.
- The flow is steady, turbulent, compressible, and
- The body force is negligible.

a) Governing Equations

The vortex tube's swirling fluid flow is regulated by non-linear partial differential equations of mass balance, momentum balance, energy balance, turbulence model, and ideal gas equations. These equations can be modelled mathematically using the following notation:

International Journal of Engineering Research & Technology (IJERT)
ISSN: 2278-0181
Vol. 11 Issue 07, July-2022

1. Conservation of Mass Equation:

$$\frac{\partial \rho}{\partial t} + \nabla.(\rho u) = 0 \quad (5)$$

2. Momentum Balance Equation:

$$\frac{\partial(\rho u)}{\partial t} + \nabla.(\rho u u) = \nabla p + \mu \nabla^2 u \quad (6)$$

3. Energy Balance Equation:

$$\rho C_p \left[\frac{\partial T}{\partial t} + \nabla.(uT)\right] = k\nabla^2 T \quad (7)$$

4. Ideal gas law for compressible flow:

$$\frac{P}{\rho} = RT \quad (8)$$

5. Turbulence Model (Standard *k-e*)

5.1 For Turbulence Kinetic Energy, *k*

$$\frac{\partial(\rho k)}{\partial t} + \frac{\partial(\rho k u_i)}{\partial x_i} = \frac{\partial}{\partial x_j}\left[\frac{\mu_t}{\sigma_k}\frac{\partial k}{\partial x_j}\right] + 2\mu_t E_{ij}E_{ij} - \rho\varepsilon \quad (9)$$

5.2 For Dissipation, *ε*

$$\frac{\partial(\rho\varepsilon)}{\partial t} + \frac{\partial(\rho\varepsilon u_i)}{\partial x_i} = \frac{\partial}{\partial x_j}\left[\frac{\mu_t}{\sigma_\varepsilon}\frac{\partial \varepsilon}{\partial x_j}\right] + C_{1\varepsilon}\frac{\varepsilon}{k}2\mu_t E_{ij}E_{ij} - C_{2\varepsilon}\rho\frac{\varepsilon^2}{k} \quad (10)$$

The k-ε model, unlike the preceding turbulence model, does not focus on processes that alter kinetic energy. The main assumption of this model is that a turbulent dynamic viscosity means that the ratio of shear stress to shear strain is the same in all fluid flow directions. Thus, the following transport equations provide the turbulence kinetic energy, k-ε and its rate of dissipation [18]:

$$\mu_t = \rho C_\mu \frac{k^2}{\varepsilon} \quad (11)$$

The terms k, ε, and C_μ indicate the kinetic energy of turbulence, the rate of dissipation, and a constant equal to 0.09, respectively.

b) Boundary conditions for vortex tube analysis

For the governing equations to be solved successfully, suitable boundary conditions are used. For the current study, the boundary conditions are as follows: - the total pressure conditions at the nozzle's intake concerning the corresponding cases.

1. The Inlet pressure is varied from 3 Bar to 7 Bar for case1, case2, and case3 respectively.
2. The outlet Pressures of 0 bar gauge and I bar gauge are applied at the cold and hot exits, respectively.
3. The wall is considered to be adiabatic with no Slip condition.
4. No-slip condition for all directions on the wall

As the cold mass fraction is regulated, by partly closing the control valve because of that there is an increase in the air pressure (rises above the outside pressure) at the hot end, so the higher pressure (i.e.one bar gauge) is applied at the hot exit whereas zero bar gauge pressure is applied at the cold outlet.

III. RESULTS OF NUMERICAL ANALYSIS

This section provides an explanation of the mechanism of energy separation based on numerical simulation and a full parametric analysis of critical design factors that directly impact the thermal performance of the vortex tube. The results and discussions of numerical analysis are done by observing the pressure and temperature drop with the energy separation inside the vortex tube. Some of the characteristics that have been studied also included the supply pressure, control valve parameters, and hot and cold gas mass percentage. Where isothermal and constant heat flux wall boundaries have been taken into consideration, the impact of the thermal environment on the performance of the vortex tube is also explored.

The simulations are conducted to determine the best conditions necessary for the cold box with respect to case1, case2, case3, and that are for 2, 4, and 6 nozzles accordingly, with various subcases depending on inlet pressure at 3, 4, 5, 7 bar. In this scenario, the basic requirement of temperature is around 276k at the cold end as an output, so to get that, a vortex tube simulation is performed to acquire minimum temperature drop and pressure decrease.

A. Results for Cold End (Minimum) and Hot End (Maximum) Temperatures:

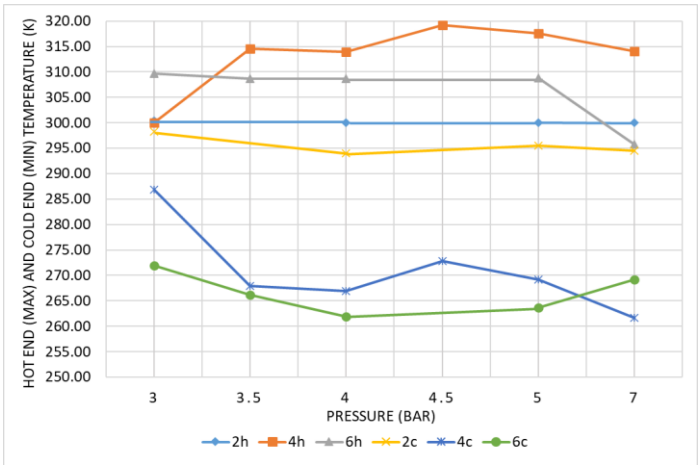

Fig. 7. Simulation result of the change in the cold end (minimum) and hot end (maximum) temperatures.

In Fig. 7, 2h, 4h, and 6h depict hot end temperatures with respect to 2,4,6 bar pressure, while 2c, 4c, and 6c depict cold end temperatures with the number of inlet nozzles. From Fig. 7, because of the minimum and maximum temperature conditions, it is not possible to determine the optimum parametric condition for the cod box RCB 503L. To do so, average temperatures on both ends can be taken into consideration (as shown in Fig. 8).

B. Results for the Average Temperatures at Cold and Hot End with varying pressure inlet.

Fig. 8 shows the average temperature at the cold end the vortex tube for number of nozzles 2, 4 and 6, as 2c, 4c and 6c with varying pressure inlet. Similarly for the average temperature at the hot end the vortex tube for number of nozzles 2, 4 and 6, is shown by 2h, 4h and 6h with varying pressure inlet. In Case 2, the temperature difference rises steadily as the pressure is increased, just as it would in a perfect situation. But in case3 (of 6 intake nozzles), temperature values progressively rises and peak at 4 bar when incoming air from the nozzle starts to thermally contaminate

International Journal of Engineering Research & Technology (IJERT)
ISSN: 2278-0181
Vol. 11 Issue 07, July-2022

the cold air at the cold end due to increasing supply pressures. Hence, at 5 and 7 bar, the temperature difference decreases. Thus, we get the optimum condition at 4 bar for 6 nozzles and this condition will be considered for further design on cooling box.

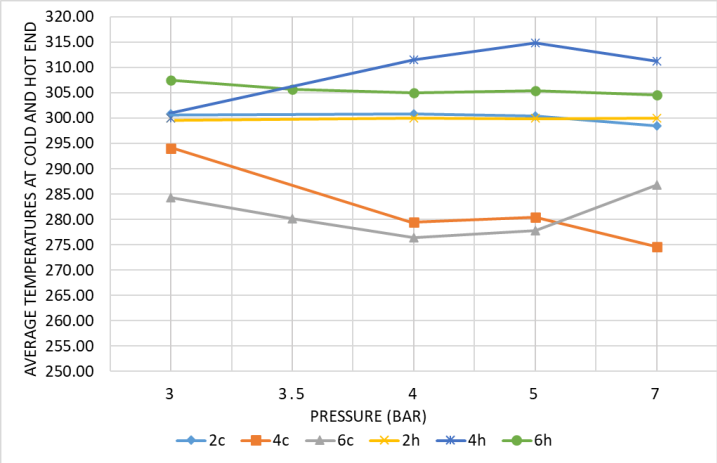

Fig. 8. Simulation result of cold end and hot end average temperatures.

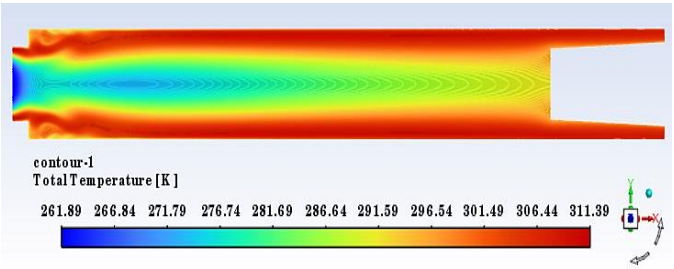

Fig. 9 Total temperature contour for subcase3.2 - 6 nozzles at 4 bar

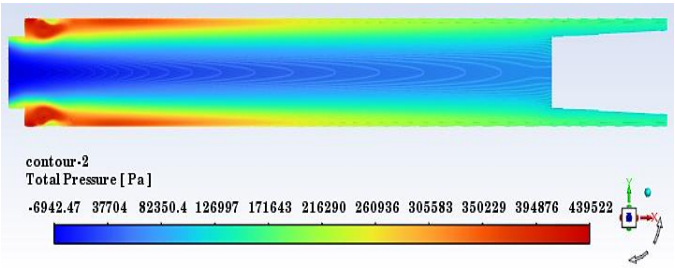

Fig. 10. Total pressure contour for subcase3.2 - 6 nozzles at 4 bar

C. *Temperature and Pressure Distribution of the Vortex Tube (For Optimum Case):*

The temperature and pressure contours in Fig. 9 and Fig. 10, which are represented on a longitudinal mid-cutting plane that passes through the mid axis, support the energy separation phenomenon caused by the expansion of supplied air.

In this optimum subcase3.2 (6 nozzles at 4 bar), required temperature conditions are satisfied i.e., 276K at cold end. As further, increasing inlet pressure above the optimal pressure, resulted in thermal contamination at the cold end outlet. As a result, at 5 and 7 bar intake pressure, the total temperature differential is reduced.

A cooled plume is observed concentrating in a narrow region near the cold exit. The hot air has taken over most of the area, including the stagnation area surrounding the control valve. The hottest pocket at the inlet is formed by viscous heat in the trapped gas. The wall temperature is seen to rise up to a particular downstream length before falling from entry to hot exit. This is due to faster energy diffusion towards the bulk of the fluid approaching the stagnation zone. The temperature of the centerline fluid is falling as it approaches the cold end.

As a result, the majority of the energy separation occurs towards the cold end, which is less than 50% the tube length. The peripheral flow is characterized by strong swirling flows with a high level of tangential velocity, which acts as a heating source and consumes the majority of the cooling effect provided by the expansion effect, while also adding heat to the peripheral fluid, this causes hot fluid to escape from the hot end. The pressure distribution is also shown in a mid-plane throughout the length of the tube. A variation in pressure gradient also be seen in axial and radial directions of flow.

D. *Grid Independence Test:*

To reduce the computational errors caused by the coarseness of the grids, this grid independence study has been performed on a variety of cell counts.

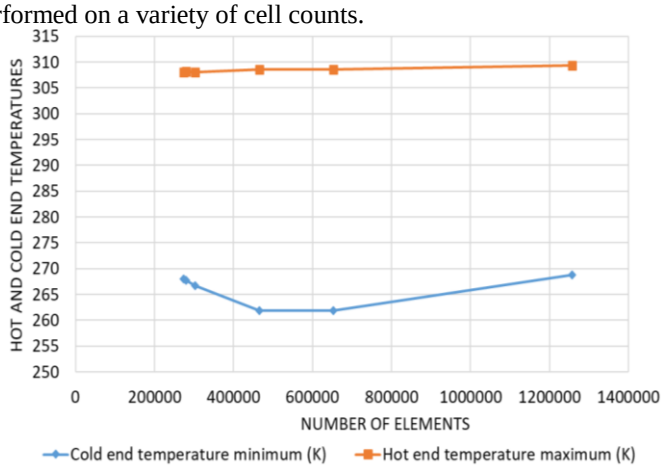

Fig. 11. Effects of Mesh Density on the temperatures at Cold and Hot End for Subcase3.2.

The present work uses, ANSYS mesh software to generate structured mesh with inflation. This grid independence study is carried out for the optimum subcase3.2 (with 6 nozzles and 4bar). Analysis of hot and cold end temperatures is also carried out to confirm that the results obtained are independent of the mesh density.

As shown in Fig. 11, the hot and cold end temperatures are varied for various numbers of cells and the sizes of the cells ranged from 274,148 to 1256870. For a cell size of 123,598, the cold side temperature approached an optimal condition. It is noticeable that there really is no significant change in the hot and cold end temperatures after 652,564 elements i.e., 0.4mm element size.

E. *Validation of work:*

The majority of the research is limited to validating the optimized vortex tube model using experimental data, and the developed models are not utilised to predict device performance in scenarios when experimental data unavailable. As a result, the validation of this research of optimized vortex tube model with optimal case and pressure condition (i.e., at 4bar) is shown in Fig. 12 and Fig. 13.

International Journal of Engineering Research & Technology (IJERT)
ISSN: 2278-0181
Vol. 11 Issue 07, July-2022

Fig. 12 depicts the effect of altering hot mass fraction on cold exit temperature and hot exit total temperature difference. Regulating the cone valve flow varies the hot Mass fraction and Temperatures decrease as hot mass fraction increases. And as in Fig. 13, the cold mass fraction with respect to cold temperature difference is shown. There is a close match between numerical and experimental work by Behera et al. [28], in with less than 6% inaccuracy is found in this comparison work.

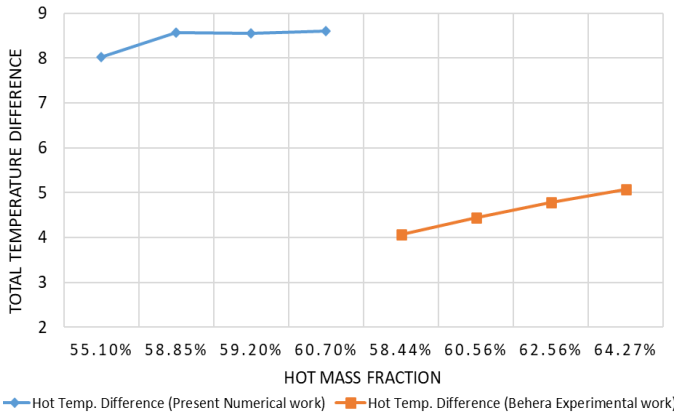

Fig. 12. Validation of the study for Hot mass fraction

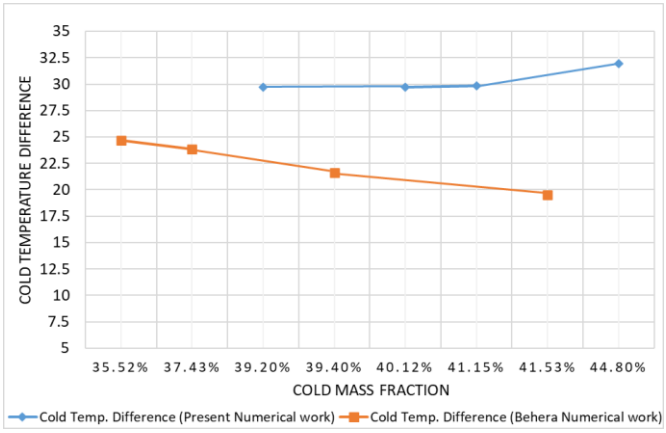

Fig. 13. Validation of the study for Cold mass fraction

IV. AMALGAMATION OF VORTEX TUBE AND VACCINE COLD BOX:

In accordance with the objective, here developed a cooling system for a vaccine container that uses vortex tube refrigeration. As shown in this structural diagram (Fig. 14), a self-sustained cooling system with the amalgamation of Exair Model 3208 Vortex tube [20], and RCB 503L vaccine container [23], with cooling coil is shown. All of these components are connected together by using flexible pneumatic connection hoses and a copper cooling coil, which helps to evenly circulate air and to maintain a temperature of 276K inside the cold box. A flexible pneumatic connecting hose connects a compressed air supply to the vortex tube's intake, and the cold flow output of a vortex tube is connected to the cooling coil inlet which is placed inside the cold box. The cooling coil receives cold air from the vortex tube and helps to keep the cold box at the desired temperature with minimum temperature fluctuations. As cold air passes through the coil and into the cold box, the Lab Armor Beads in the close surroundings (inside the cold box) are cooled. Lab Armor beads with high heat capacity ensure that the required temperature (276k) is maintained inside the cold box for an extended period of time.

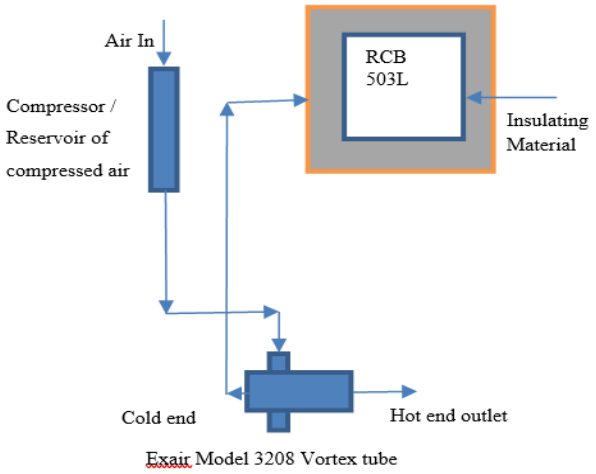

Fig. 14. Design of Cooling system

The cooling coil is attached to the left side of the vortex tube for even circulation of cold air inside the cold box. As the front and back sides of the box primarily offer support to the cold box and the heat loss is greater on these sides, so it is more advantageous to mount the cooling coil to the left side of the cold box.

A. Physical modelling of the cold box with cooling coil:

The primary function of this cooling coil is to maintain a steady and constant temperature within a cold box. As a result, its length is a crucial factor. As a result, all the calculations for the cooling coil length have been completed in below section.

1) Cooling coil design:

TABLE I. COOLING COIL DESIGN PARAMETERS

Parameters	***Values***
Diameter of cooling coil (dm)	0.0064m
Flow Area of the tube (Ac)	3.2169×10^{-5} m^2
Inlet air Temperature (T_{Ci})	276K
Mass flow rate at cold end of the vortex tube ($\dot{m}$)	0.0067258 Kg/sec
Air mean specific heat capacity (C_{PC})	1006.43 J/KgK
Density of air (ρ_C)	1.225 Kg/m^3
Axial velocity at cold end of vortex tube (ut)	0.037979 m/sec
Overall heat transfer coefficient (U)	0.2959 W/m^2K
Total cooling load (Q_{Ct})	84.087 W

From the heat balance equation:

$$Q_{ct} = \dot{m}_i C_{Pc}(T_{Co} - T_{Ci}) \quad (12)$$

$$T_{Co} = \frac{Q_{ct}}{\dot{m}_i C_{Pc}} + T_{Ci} \quad (13)$$

$$T_{Co} = 288.42k \quad (14)$$

To find the necessary length of the cooling tube, therefore, for number of tubes (N_t):

$$\dot{m}_i = \left(\rho_c A_c u_t\right).N_t \quad (15)$$

International Journal of Engineering Research & Technology (IJERT)
ISSN: 2278-0181
Vol. 11 Issue 07, July-2022

$$N_t = \frac{\dot{m}_i}{\rho_c A_c u_t} \quad (16)$$

$$N_t = \frac{\dot{m}_i \times 4}{\rho_c \pi {d_m}^2 u_t} \quad (17)$$

$$N_t = 4494.33 \quad (18)$$

$$N_t \approx 4495$$

As, heat transfer surface area (A_O) can be obtained from Equation:

$$Qc = UA_o\,(\Delta T_m) \quad (19)$$

$$A_o = \frac{Qc}{U\,(\Delta T_m)} \quad (20)$$

$$A_o = 22.8803\ m^2 \quad (21)$$

Therefore,

$$L = \frac{A_o}{(\pi d_m) \times N_t} \quad (22)$$

$$L = 0.2531\ m \quad (23)$$

From above calculations, it is clear that the optimum cooling coil length is 253.164mm i.e., approximately 254mm per pass.

B. Geometric modelling:

The Vortex tube is equipped with a cold box and a cooling coil measuring 254 mm in length per pass and 6.4mm in diameter with thicknesses of 1mm.

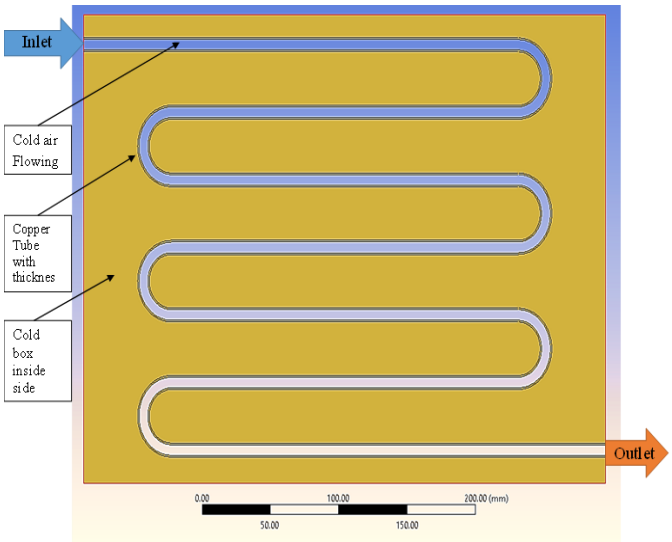

Fig. 15. Schematic inner space of the cold box RCB 503

The spiral coil's inlet end is connected to the vortex tube's cold end (at temperature of 276K). The cooling coil has a total of seven turns, and as the spiral copper tube's axial length or net length is 2808.32mm. Below is a schematic created using AUTODESK software that shows the actual coil design for the cold box RCB 503L.

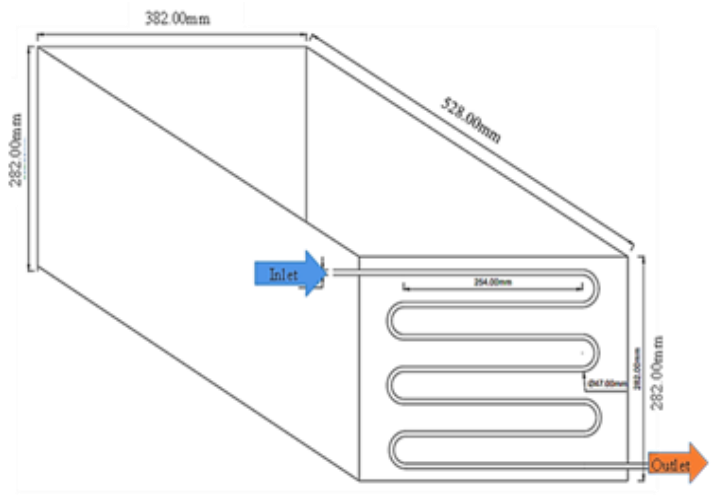

Fig. 16. 2d geometry of cold box and cooling tube amalgamation.

C. Meshing model:

The ANSYS mesh 2021R2 is used as meshing tool, to generate the mesh. For this meshing operation, an element size of 1mm is considered for overall geometry, with that face meshing is utilized on various parts of 0.5mm element size to generate a refined and structured mesh.

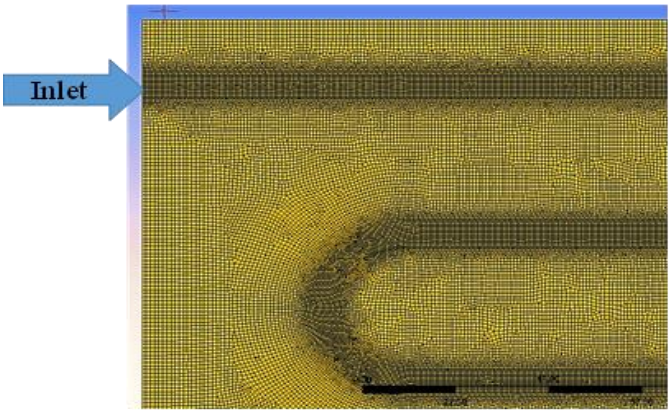

Fig. 17. Mesh on cooling coil

D. Boundary conditions:

Actual cooling coil boundary conditions are employed in this study, with a mass flow rate of 0.00673kg/sec at a temperature of 276K at the air flow input and a pressure outlet of 0-gauge bar at the air flow out. The wall is considered to be in an adiabatic state. It is established that no-slip conditions are excellent next to hard walls because of the viscous effect.

E. Results:

Results are obtained for transient case by applying above boundary conditions. For this simulation coupled solution method is utilized, the transient analysis is carried out in order to optimize systems performance. In this transient analysis the whole system i.e., cooling coil on the side face of the cold box is observed for 5 minutes.

International Journal of Engineering Research & Technology (IJERT)
ISSN: 2278-0181
Vol. 11 Issue 07, July-2022

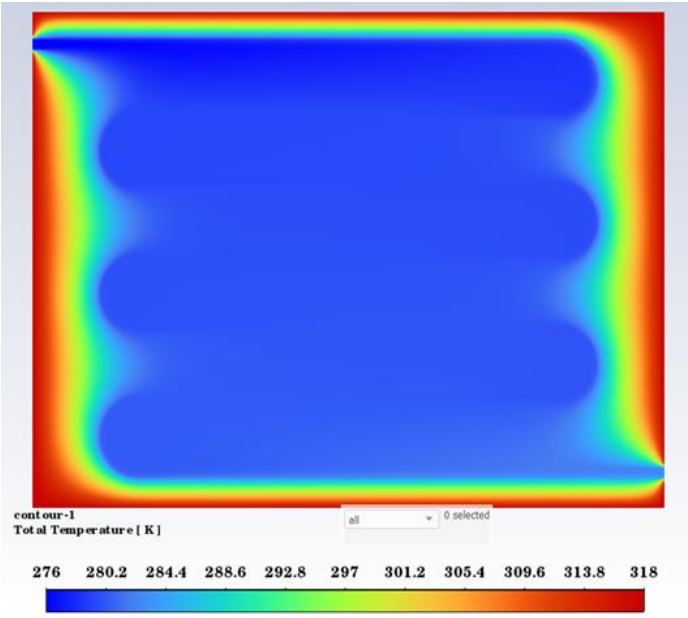

Fig. 18. Temperature contour of transient state

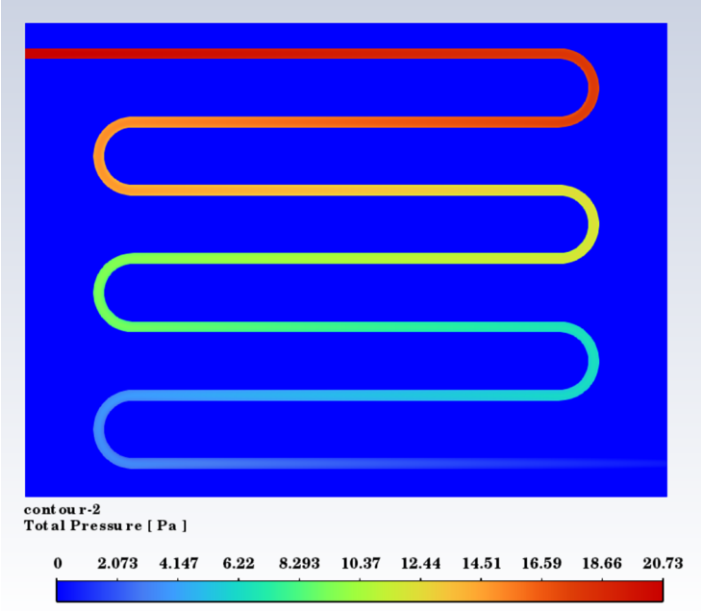

Fig. 19 Pressure contour of transient state

The above Fig. 18,depicts that during the cooling process, the transient temperature contours with a somewhat uniform temperature distribution along the side of the cold box RCB 503L. On the mid-section of the wall, temperature distribution along the coil is uniform and rather effective, while the temperature at the wall border is unaffected by the cooling coil. It is possible to lower the wall boundary temperature if precooling is provided for the container. In Fig. 19, it is clear that pressure is decreasing with the continuous flow inside the coil.

V. CONCLUSION

This study provides a solution to the current global challenge. According to studies, up to 10% of vaccines can be lost during transport due to temperature variations during storage. In places where power is unavailable, it is difficult to do continuous and long-term refrigeration to maintain the optimal temperature range of 2 to 8°C for vaccine storage. As a solution to this problem, this study proposes the vortex tube refrigeration system, which is simple, compact, and environmentally benign owing to the usage of natural refrigerant. The system is capable of chilling the cold box and maintaining the required temperature as needed by creating and maintaining a steady cool, dry atmosphere.

To design and develop a cooling system for the vaccine cold box/container, the most efficient modern thermal container, the RCB 503L, is selected, and based on the RCB 503L cold box cooling load calculation, the EXAIR Vortex Tube 3208 model is selected. With that the parametric analysis of EXAIR Vortex Tube is performed in ANSYS FLUENT 2021R2 to optimize the vortex tube design and operating parameters to acquire the required outlet temperature of 276K from the vortex tube and feed it into the cooling coil.

A. Effect of number of inlet nozzles

In all cases, raising the vortex tube's input pressure lowers the cold air temperature, while increasing the number of nozzles raises it. When the number of nozzles is four and the intake pressure is 7 bar, the minimum temperature is achieved. In case1 that is 2 nozzles and minimum pressure, and the energy separation is not in efficient way.

B. Effect of Inlet Pressure

To determine the influence of input pressure, the intake pressure (gauge) is changed from 3 to 7 bars. As can be observed in Fig. 8, the overall temperature difference increases with increasing inlet pressure, reaches a maximum value, and then begins to decrease. The increasing radial static pressure, which allows for greater expansion, and can be associated with the increase temperature difference. Incoming air from the nozzle begins to pollute the cold air at the cold end thermally at increasing supply pressures. This causes a reduction in overall difference in temperature between 5 to 7 bars.

C. Optimal solution

As a result of the analysis and the simulation, the optimum number of input nozzles for the cold stream condition for the present vortex tube design is determined to be about 6. Also, it can be seen from Fig. 7 that by utilizing minimal pressure energy (4 bar), the lowest temperature at the cold end, (which is 276.4K) with 6 nozzles and 4 bar pressure (Fig. 9) is achieved. It is the most acceptable and optimum case for the cold box RCB 503L.

As that cold temperature produced by the vortex tube cooling is fairly low, and the interior temperature within the cold box varies somewhat from one corner to the other due to a high-speed intake air therefore for efficient and uniform cooling of the cold box the cooling coil length calculations are done, with that the cooling coil and cold box side is observed under transient analysis as shown in Fig. 18 and Fig. 19.

VI. REFRENCES

[1] *S. G. Voronchikhin and M. A. Tuev, "A Mobile Medical Thermostatic Unit Based on the Ranque–Hilsch Vortex Effect" Biomedical Engineering, SpringerLink,vol. 52. , pp. 361–364, Jan. 17, 2019.*

[2] *T. K. Sharma, G. A. Prasad Rao, and K. M. Murthy, "Numerical Analysis of a Vortex Tube: A Review",Archives of Computational*

International Journal of Engineering Research & Technology (IJERT)
ISSN: 2278-0181
Vol. 11 Issue 07, July-2022

Methods in Engineering, vol. 24, no. 2017 , pp. 251–280, Jan. 16, 2016.

[3] *G. F. Nellis and S. A. Klein, "The Application Of Vortex Tubes to Refrigeration Cycles." International Refrigeration and Air Conditioning Conferenc, West Lafayette, Paper No.. 537-, Jan. 01, 2002.*

[4] *Xiaojie Zhai, "Research on the application of vortex tube type of cooling jacket in coal mine," vol. 1864, no. 1. AIP Publishing, pp. 020220-, Aug. 03, 2017.*

[5] *A. S. Bidwaik and S. M. Dhavale, "To Study the Effects of Design Parameters on Vortex Tube with CFD Analysis" IJERT., vol. 4, no. 10. pp. 90, Oct. 10, 2015.*

[6] *C. Somerton, "ASEE PEER - An Appropriate Technology Project: A Solar Powered Vaccine Refrigerator." Annual Conference & Exposition., pp. 15–140, Mar. 10, 2015.*

[7] *D. Ramakanth, S. Singh, P. K. Maji, Y. S. Lee, and K. K. Gaikwad, "Advanced packaging for distribution and storage of COVID-19 vaccines: a review" Environmental Chemistry Letters.,vol. 19, no. 5., pp. 3597–3608, Jun. 03, 2021.*

[8] *B. Ahlborn, J. U. Keller, R. Staudt, G. Treitz, and E. Rebhan, "Limits of temperature separation in a vortex tube" IOPscience., vol. 27, no. 3. IOP Publishing Ltd, pp. 480-, Mar. 14, 1994.*

[9] *B. S. Kumar Reddy and K. Govindarajulu, "Air Cooling in Automobiles Using Vortex Tube Refrigeration System" Trans Tech Publications., vol. 592–594., Scientific.Net, pp. 1408–1412, Jul. 15, 2014.*

[10] *M. F. Bakhsheshi, Y. Wang, L. Keenliside, and T.-Y. Lee, "A new approach to selective brain cooling by a Ranque-Hilsch vortex tube",Intensive Care Medicine Experimental., vol. 4, no. 1. , pp. 1–14, Sep. 29, 2016.*

[11] *Metodiev, K., L. Vigani, R. Plackett, K. Arndt, D. Wood, D. P. Weatherill, M. Mironova, D. Bortoletto, and I. Shipsey, "A compact air cooling system for testing silicon detectors based on a vortex chiller", ScienceDirect., vol. 940, pp. 405–409, Jul. 01, 2019.*

[12] *W. Rattanongphisat, "Efficiency of Vortex Tube Enclosure Cooling ", Scientific.Net., vol. 666. Trans Tech Publications Ltd., pp. 154–158, Oct. 20, 2014.*

[13] *Majidi D, Alighardashi H, Farhadi F. "Best vortex tube cascade for highest thermal separation," vol. 85. pp. 282–291, Oct. 18, 2017.*

[14] *Promvonge, P. and Eiamsa-ard, S., "Investigation on the vortex thermal separation in a vortex tube refrigerator", Science Asia, vol. 31, no. 3, pp.215-223.,Apr. 18, 2005.*

[15] *R. S. Maurya and K. Bhavsar, "Energy and Flow Separation in the Vortex Tube : A Numerical Investigation" Semantic Scholar," vol. 2, pp. 25–35, Jan. 01, 2016.*

[16] *Marques, C.H., Isoldi, L.A., Santos, E.D.D. and Rocha, L.A.O., "Constructal design of a vortex tube for several inlet stagnation pressures," vol. 11, no. 1., pp. 85–92, Jan. 01, 2012.*

[17] *Jiri linhart, Richard Matas, Mohamed Kalal," Experimental And Numerical Model Investigation Of Vortex Tube PerformanceNew Technologies Research Centre, University of West Bohemia.*

[18] *Pourmahmoud N, Akhesmeh S., "Numerical investigation of the thermal separation in a vortex tube", International Journal of Mechanical and Mechatronics Engineering., vol. 2, no.7, pp. 919-925, Jul. 23.2008.*

[19] *Anan Tempiam, Pongsakorn Kachapongkun, Phadungsak Rattanadecho, Ratthasak Prommas"Experimental investigation of vortex tube for reduction air inlet of a reciprocating air compressor - ScienceDirect," vol. 19. Elsevier Ltd., pp. 100617-, Feb. 29, 2020.*

[20] *Exair vortex, "Exair vortex tube manual" 2021.H. M. Skye, G. F. Nellis, S.A. Klein, "Comparison of CFD analysis to empirical data in a commercial vortex tube," International journal of refrigeratio., vol. 19, no. 1., pp. 71–80, Aug. 15, 2005.*

[21] *R. A. Bramo and N. Pourmahmoud, "CFD simulation of length to diameter ratio effects on the energy separation in a vortex tube," Thermal Science., vol. 15, no. 3. pp. 833–848, Jan. 01, 2011.*

[22] *H. M. Skye, G. F. Nellis, S.A. Klein, "Comparison of CFD analysis to empirical data in a commercial vortex tube," International journal of refrigeratio., vol. 19, no. 1. sciencedirect, pp. 71–80, Aug. 15, 2005.*

[23] *Nilkamal, "Vaccine cold boxes catelog," 2021.*

[24] *Rajagopalan and A. Gopal, "Geometric Modifications and their Impact on the performance of the Vortex Tube." University of Cincinnati and OhioLINK, Jan. 01, 2016.*

[25] *Bezprozvannykh, Vlad, and Hank Mottl. "The Ranque-Hilsch Effect: CFD Modeling." In Proceedings of the Eleventh Annual Conference of the CFD Society of Canada., vol. 2, pp. 651., 2003*

[26] *M.Manickam, J. Prabakaran,"Effect of number of the nozzle and cold mass fraction on the performance of counter flow vortex tube using the computational fluid dynamic analysis,"International Journal of Ambient Energy., vol. 43, no. 1., pp. 1134–1148, Aug. 07, 2019.*

[27] *Ahim Shamsoddini, Bahador Abolpour, "A geometric model for a vortex tube based on numerical analysis to reduce the effect of nozzle number," International Journal of Refrigeration., vol. 94. sciencedirect, pp. 49–58, Aug. 10, 2018.*

[28] *Upendra Behera, P.J. Paul, S. Kasthurirengan, R. Karunanithi, S.N. Ram, K. Dinesh, S. Jacob, "CFD analysis and experimental investigations towards optimizing the parameters of Ranque–Hilsch vortex tube", International Journal of Heat and Mass Transfer., ScienceDirect," vol. 48, no. 10. sciencedirect, pp. 1961–1973, Mar. 16, 2005.*